doi:10.1006/jmbi.2001.4593 available online at http://www.idealibrary.com on IDEAL® *J. Mol. Biol.* (2001) **308**, 515–525

JMB

Identification of a Novel Human Islet Amyloid Polypeptide β-Sheet Domain and Factors Influencing Fibrillogenesis

Emma T. A. S. Jaikaran[1,2]*, Claire E. Higham[2], Louise C. Serpell[3] Jesús Zurdo[4], Michael Gross[4], Anne Clark[1,2] and Paul E. Fraser[5]

[1]*Diabetes Research Laboratories Radcliffe Infirmary, Woodstock Road, Oxford OX2 6HE, UK*

[2]*Department of Human Anatomy and Genetics, University of Oxford, South Parks Road, Oxford OX1 3QX UK*

[3]*University of Cambridge Structural Medicine Unit, Cambridge Institute for Medical Research, Wellcome Trust Centre for Molecular Mechanisms of Disease, Hills Road, Cambridge CB2 2XY UK*

[4]*Oxford Centre for Molecular Sciences, New Chemistry Laboratory, University of Oxford, South Parks Road Oxford OX1 3QT, UK*

[5]*University of Toronto, Centre for Research in Neurodegenerative Diseases and Department of Medical Biophysics, Tanz Neuroscience Building, 6 Queen's Park Crescent West, Toronto Ontario, Canada M5S 3H2*

**Corresponding author*

Human islet amyloid polypeptide (hIAPP) accumulates as pancreatic amyloid in type 2 diabetes and readily forms fibrils *in vitro*. Investigations into the mechanism of hIAPP fibril formation have focused largely on residues 20 to 29, which are considered to comprise a primary amyloidogenic domain. In rodents, proline substitutions within this region and the subsequent β-sheet disruption, prevents fibril formation. An additional amyloidogenic fragment within the C-terminal sequence, residues 30 to 37, has been identified recently. We have extended these observations by examining a series of overlapping peptide fragments from the human and rodent sequences. Using protein spectroscopy (CD/FTIR), electron microscopy and X-ray diffraction, a previously unrecognised amyloidogenic domain was localised within residues 8 to 20. Synthetic peptides corresponding to this region exhibited a transition from random coil to β-sheet conformation and assembled into fibrils having a typical amyloid-like morphology. The comparable rat 8-20 sequence, which contains a single His18Arg substitution, was also capable of assembling into amyloid-like fibrils. Examination of peptide fragments corresponding to residues 1 to 13 revealed that the immediate N-terminal region is likely to have only a modulating influence on fibril formation or conformational conversion. The contributions of charged residues as they relate to the amyloid-forming 8-20 sequence were also investigated using IAPP fragments and by assessing the effects of pH and counterions. The identification of these principal amyloidogenic sequences and the effects of associated factors provide details on the IAPP aggregation pathway and structure of the peptide in its fibrillar state.

Keywords: islet amyloid polypeptide (IAPP); diabetes; amyloid fibrils; circular dichroism; electron microscopy

Introduction

Human islet amyloid polypeptide (hIAPP) is a 37 amino acid residue peptide present in pancreatic β-cell secretory granules and is co-secreted with insulin. In type 2 diabetes, hIAPP aggregates in the islet extracellular space to form fibrillar amyloid deposits (Clark *et al.*, 1987; Westermark *et al.*, 1987). These deposits are present in over 95% of type 2 diabetic subjects at post mortem and their

Abbreviations used: hIAPP, human islet amyloid polypeptide; rIAPP, rat islet amyloid polypeptide; Fourier-transform infrared spectroscopy; TFE, trifluoroethanol; HFIP, hexafluoro-2-propanol; Thio-S, thioflavin S.

E-mail address of the corresponding author: emma@drl.ox.ac.uk

0022-2836/01/030515–11 $35.00/0

abundance correlates with the severity of disease (Röcken *et al*., 1992; Schneider *et al*., 1980; Westermark & Johnson, 1988). Due to the unfolded nature and conversion of hIAPP to fibrils in aqueous media, the secondary structure of the peptide has not been determined (Hubbard *et al*., 1991; Saldanha & Mahadevan, 1991). In the presence of helix-inducing organic solvents, such as trifluoroethanol (TFE) or hexafluoro-2-propanol (HFIP), the CD spectra of hIAPP are indicative of α-helical structure (Hubbard *et al*., 1991; McLean & Balasubramaniam, 1992). However, in the absence of these solvents and with the elimination of potential ''seeds'' by filtration, the CD spectra of hIAPP in water appears initially as a random coil (Higham *et al*., 2000; Kayed *et al*., 1999). Over a period of days, the peptide either precipitates from solution as amorphous aggregates or converts to a β-sheet structure accompanied by fibril formation (Higham *et al*., 2000; Kayed *et al*., 1999).

A single amyloidogenic region spanning residues 20 to 29 has been proposed to be the important factor in fibril formation of hIAPP (Betsholtz *et al*., 1990; Glenner *et al*., 1988; Westermark *et al*., 1990). This proposal was based on the association of species-specific proline substitutions in rodent IAPP 20-29, which prevents fibril formation. This single β-strand fragment was shown to form intermolecular hydrogen bonds and β-sheets (Griffiths *et al*., 1995). However, recent studies have identified a second potential amyloidogenic region within residues 30 to 37, which forms amyloid-like fibrils in aqueous media (Nilsson & Raleigh, 1999). With the presence of more than one β-strand region, intermolecular interactions as well as intramolecular interactions involved in fibril formation are likely to be more complex than that proposed for the single-strand region, IAPP 20-29 (Griffiths *et al*., 1995).

These two amyloidogenic domains account for approximately half of the IAPP molecule (C-terminal residues 20 to 37) and it is unclear what contributions to fibril formation may be made by the remaining N-terminal domains (residues 1-20). We have used CD, EM, Fourier transform infrared spectroscopy (FTIR) and fibre X-ray diffraction to examine the structure and fibril assembly of a series of IAPP fragments. These peptides spanned the entire length of IAPP and were derived from both the human and rat sequences. This permitted a comparative study of the two distinct portions of IAPP (N *versus* C-terminal domains) and the effects of subtle changes in sequence (e.g. His18Arg substitution) on peptide aggregation. In addition, the N-terminal half of IAPP (residues 1-20) has a number of unique features that may affect folding and/or aggregation. Our observations indicate that a novel amyloidogenic β-sheet domain is contained within residues 8 to 20 and may represent a core structural element of the fibril.

Results

Secondary structure predictions of IAPP domains

Secondary structure predictions using a computer algorithm (Deleage & Roux, 1987) indicate that there are three potential β-strand regions in the human IAPP (hIAPP). These include the previously described fibrillogenic region contained within residues 20 to 29 and two additional domains that may contribute to amyloid formation (Figure 1). The first is located at the C terminus (residues 30-34) and the second encompassing residues 14 to 18. It has been reported that peptides derived from the C terminus, residues 30 to 37, assemble into amyloid-like fibrils having a β-sheet conformation (Nilsson & Raleigh, 1999). The contribution of the IAPP N-terminal domain (residues 1-20) has yet to be resolved but the predictive algorithms suggest that the central region from approximately Asn14 to His18 may assemble into a β-conformation (Figure 1). The remainder of IAPP spanning approximately the first 15 residues is predicted to be either random coil or α-helical.

Folding and aggregation of the C-terminal domains (20-29 and 30-37) are most likely driven by hydrophobic interactions. The fact that the 20-29 and 30-37 sequences represent distinct amyloidogenic domains is based upon the previous identification of 20-29 as a key fibre-forming region (Westermark *et al*., 1990). The 30-37 domain is supported by *in vitro* peptide studies (Nilsson & Raleigh, 1999) as well the secondary structure analyses. It is conceivable that the C terminus, spanning residues 20 to 37, is a contiguous β-sheet strand and additional studies are required to address this possibility. In contrast, the N-terminal sequence contains a number of unique features such as a disulphide bridge that terminates before the first predicted β-strand. An intact disulphide bridge has been proposed to be essential for the physiological function of IAPP (Roberts *et al*., 1989) but it is unclear if the bridge remains intact in amyloid fibrils. This region contains all of the IAPP electrostatic residues (Lys1, Arg11 and His18), which may influence peptide folding and aggregation. This region also has a His/Arg substitution (Figure 1, arrow) in the non-amyloidogenic rodent sequence. Histidine residues play an important role in Aβ fibril formation (Fraser *et al*., 1994). Their protonation state can regulate β-sheet folding and facilitate zinc binding, which can enhance peptide aggregation and is found at high concentrations in the β-cell secretory granule (Emdin *et al*., 1980).

Conformation analysis of IAPP and its peptide fragments

To test these predictions, a series of peptides corresponding to fragments of human and rat IAPP (rIAPP) were examined. These included the

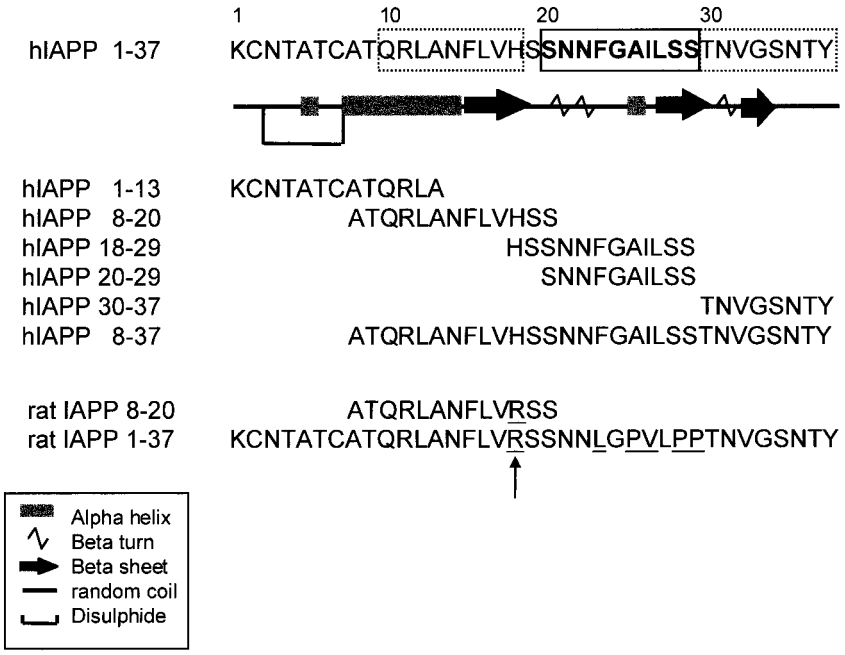

Figure 1. Secondary structure predictions and amyloidogenic domains of human and rat IAPP. Secondary structure prediction for human IAPP by double prediction algorithm (Deleage and Roux, 1987) identified three principal β-sheet domains. These corresponded to residues 20 to 29 (highlighted), 30 to 37 and ~10 to 20. Amino acid sequences are shown for the human and rat IAPP peptides that were investigated. Sequence divergences between human and rat, such as the His18Arg (arrow) and proline substitutions (underlined) are indicated.

N-terminal fragments (residues 1-13 and 8-20), which were compared to C-terminal fragments (residues 20-29 and 30-37), overlapping sequences (residues 18-29 and 8-37) and full-length IAPP, residues 1 to 37. To establish identical starting conditions for examining fibril formation, all peptides were first solubilised in 100% HFIP, filtered (0.2 μm), and freeze-dried in aliquots, which were reconstituted in water or buffer as required (100 μg/ml). These conditions have been shown to maintain full-length hIAPP 1-37 in a soluble random conformation that undergoes a slow transition to the amyloidogenic β-sheet (Higham *et al*., 2000).

Under these conditions, all peptides initially demonstrated a CD spectrum typical of a random coil conformation most likely representative of the monomeric state (Figure 2). Following incubation at room temperature for 48-96 hours, the fragments displayed a number of different folding properties. The N-terminal peptide (residues 1-13) remained as a random coil, even following extended incubation and under a variety of conditions (Figure 2(a)). This is consistent with the predicted conformation, where this domain is largely a disordered and flexible region of IAPP. One possibility is that the N-terminal sequence may modulate folding rather than contribute to fibril formation. In contrast, the IAPP 8-37 fragment folded into a typical amyloidogenic β-sheet conformation, similar to that observed for the intact IAPP 1-37 (Figure 2(b)). This N-terminal truncated fragment, lacking the disulphide bridge, assembled into fibrils that had a morphology identical with that of the full-length peptide (data not shown).

The other potentially amyloidogenic domain was predicted within the region of hIAPP residues 14-18 and to assess this possibility, the peptide fragment spanning Ala8-Ser20 was examined. The CD investigation indicated that the hIAPP 8-20 was initially in a random coil conformation similar to that of the other peptides examined (Figure 2(c)). However, following incubation, the signal did not convert to a typical β-sheet but instead merely diminished in intensity (Figure 2(c)). This attenuation was most likely due to a precipitation of the peptide following aggregation. Varying other conditions, such as the peptide concentration to 1 mg/ml, did not significantly alter the CD spectra or the precipitation rate of the peptide aggregates (data not shown). A similar observation was made with the more hydrophobic IAPP 30-37 fragment, which also appeared to undergo a rapid aggregation and precipitation (data not shown). Although these findings suggest that hIAPP 8-20 may display a tendency to aggregate into amyloid-like fibrils, it was not possible to ascertain by CD spectroscopy if the precipitate was in a β-conformation. To resolve this problem, the IAPP 8-20 fragment was examined by other techniques that are more amenable to the solid state.

Fourier-transform infrared (FTIR) spectroscopy was used to evaluate the conformation of the human and rat IAPP 8-20 peptide fragments. These peptides displayed similar spectra, with absorbance maxima at 1618-1620 cm^{-1} typical of intermolecular β-sheet conformation (Figure 2(d) and (e)) as was reported for amyloid-β (Aβ) (Fraser *et al*., 1991; Surewicz *et al*., 1993). Some additional absorbance was observed at 1662-1664 cm^{-1} and 1648 cm^{-1} that could arise from turns/bends and random contributions, respectively. However, these were relatively minor, which suggests that the peptides adopted an almost exclusively β-sheet conformation. Whilst the full-length rat IAPP pep-

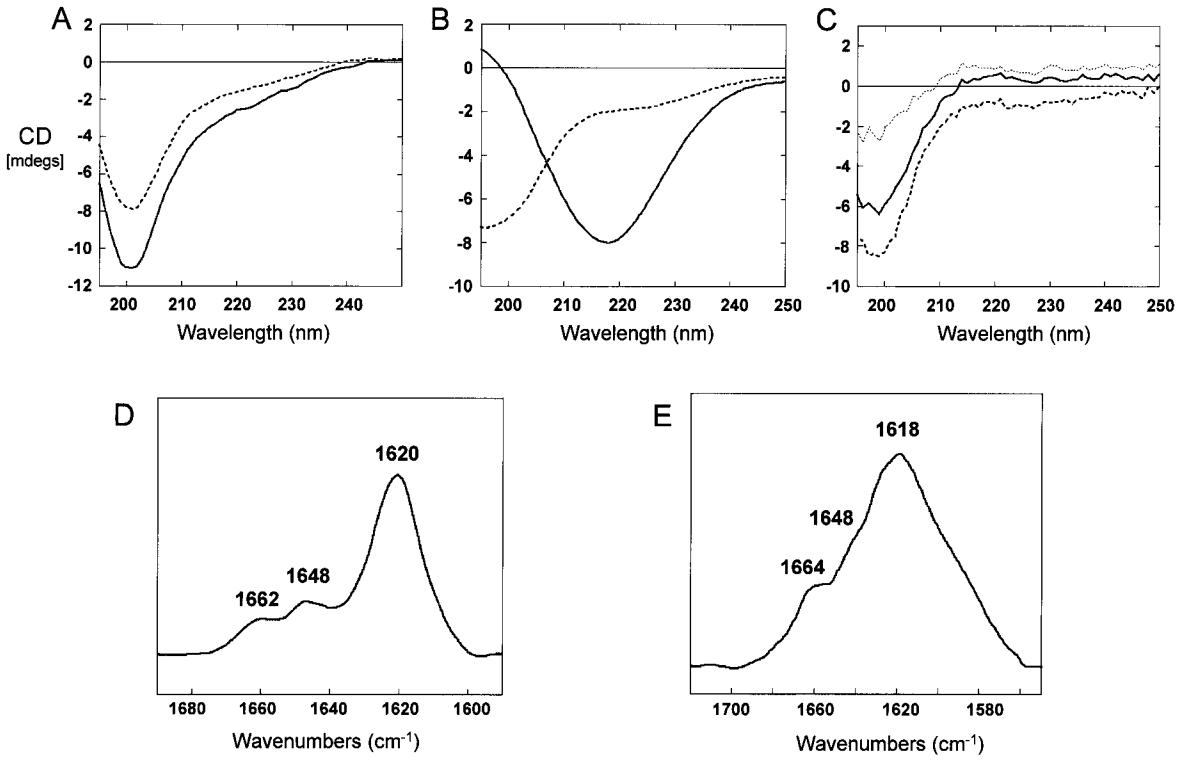

Figure 2. Conformation of IAPP peptides assessed by protein spectroscopy. (a) CD of human IAPP residues 1-13 in 10 mM sodium acetate buffer pH 5.5. This fragment appeared as a random coil conformation at time 0 (broken line), which did not change with time (96 hours incubation, continuous line). (b) IAPP residues 8 to 37 displayed folding properties similar to the full-length human peptide; the initially random structure (broken line) underwent a transition to β-sheet (continuous line) following 48 hours incubation. (c) CD spectra for hIAPP 8-20 in water indicated a random coil conformation at time 0 (broken line) that gradually diminished in intensity following incubation for 96 hours (continuous line) and four weeks (dotted line). (d) FTIR spectrum of rat IAPP 8-20 after incubation showed β-sheet conformation with a peak at 1620 cm^{-1}. (e) A comparable FTIR spectrum was obtained with the human IAPP 8-20 with a clear β-structure as indicated by the absorbance at 1618 cm^{-1}.

tide has been shown by several groups to be non-amyloidogenic (e.g. see Betsholtz *et al.*, 1989), it appears that the 8-20 domain is capable of assembling into an amyloidogenic structure. The human and rodent 8-20 sequences are identical except for of an His/Arg substitution at position 18 (see Figure 1).

The amyloidogenic potential of the 8-20 region was further examined by fibre X-ray diffraction and thioflavin S (Thio-S) staining. Amyloid X-ray diffraction studies have demonstrated that the fibrils assemble into a cross-β organization that may represent a common structure (Sunde *et al.*, 1997). The full-length IAPP (1-37) displays a similar structure, as shown by the orthogonal arrangement of the intersheet (~10 Å) and hydrogen-bonding (4.7 Å) reflections (Figure 3(a)). Examination of the hIAPP 8-20 fragment revealed a similar set of reflections that are consistent with a β-sheet fibril (Figure 3(b)). However, the fibrils did not orient as well as the full-length IAPP, possibly due to the tendency of this fragment to aggregate rapidly. The amyloid-like nature of the human and rat IAPP 8-20 aggregates was demonstrated further by their staining with Thio-S. This histological dye, like Congo red, is considered to be specific for β-sheet fibrils and is an indirect indication of amyloidogenic conformation (Schwartz, 1970). Human IAPP 8-20 showed the characteristic apple-green birefringence with Congo red staining and the typical yellow fluorescence of Thio-S binding (Figure 3(c)). A similar staining was obtained with the rat IAPP 8-20 fragment. Together, these data indicate that the 8-20 region contains a previously unrecognised amyloidogenic domain. This section of IAPP may therefore act in combination with the other known fibril-formation sequences (i.e. 20-29 and 30-37) to facilitate folding and aggregation of the full-length human IAPP.

Fibril formation and morphology of IAPP amyloidogenic domains

The morphology of the aggregated IAPP peptide fragments was examined by negative stain electron microscopy. Examination of the IAPP 1-13 fragment under several conditions did not result in any detectable aggregate. This is consistent with the random coil conformation observed by CD spectroscopy. In contrast, the IAPP 8-20 peptides

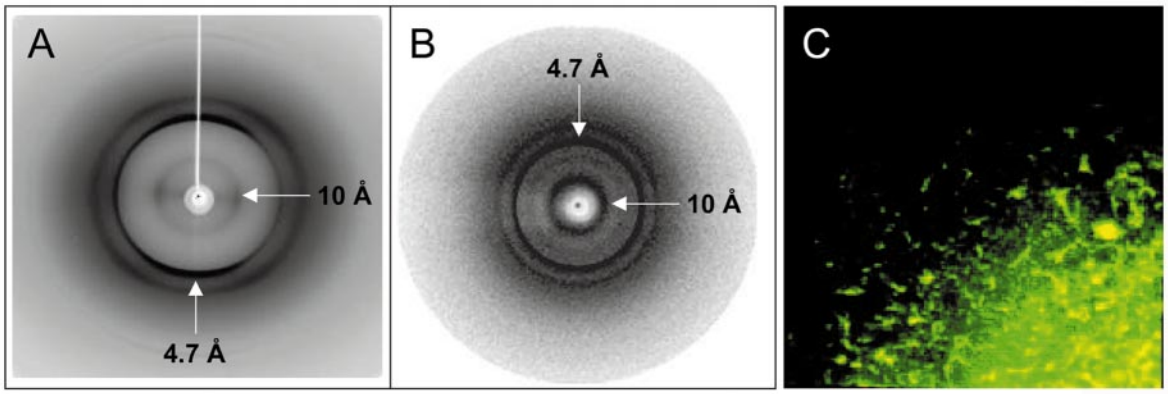

Figure 3. Structure of IAPP and its amyloidogenic fragments. Fibre X-ray diffraction of (a) full-length IAPP 1-37 and (b) the N-terminal amyloid domain, residues 8-20. The aligned IAPP 1-37 fibrils oriented sufficiently to reveal the typical cross-β structure with the equatorial intersheet spacing (~10 Å) and the intense meridional hydrogen bonding reflection (4.7 Å). The IAPP 8-20 did not orient but displayed a comparable β-sheet diffraction pattern. (c) The amyloid-like properties of the human IAPP 8-20 fragment was also demonstrated by Thio-S staining and similar staining was observed with the corresponding rat sequence (not shown).

exhibited a well-defined fibrillar organisation, which was formed concurrently with the attenuation of its CD signal (Figure 4(a)). Overall, the fibrils had a ribbon-like appearance, which seemed to result from the lateral association of individual protofilaments to produce structures with widths of 18-20 nm. This was more evident at higher magnification, where distinct fibrils with an approximate diameter of 8-9 nm could be resolved within the ribbon structures (Figure 4(a), inset). The constituent fibrils were similar in appearance to those formed from full-length IAPP but have a greater propensity to associate laterally, possibly due to the absence of the other modulating domains. A similar morphology was observed for the rat IAPP 8-20 fragment (Figure 4(b)).

Fibrils formed from IAPP 8-20 were compared to those formed from the other amyloidogenic domains. A slightly overlapping fragment, IAPP 18-29, containing the histidine, formed rod-like structures, although some longer fibrils and loose networks were observed (Figure 4(c)). IAPP 30-37 showed non-fibrillar precipitates and these amorphous aggregates could not be solubilised even under harsh conditions (e.g. 10 mM HCl). This precipitated material was capable of acting as a nucleus for fibrillogenesis, as fibres with a typical appearance appeared over time but were also associated with amorphous material (Figure 4(d)). However, the IAPP 30-37 fibrils had a relatively small diameter (~6-7 nm) and aggregated laterally into dense networks. These observations indicate that the primarily C-terminal β-sheet domains (20-29 and 30-37) do not assemble into typical amyloid-like fibrils. In contrast, the constituent fibrils of the human and rat 8-20 fragments displayed a morphology more consistent with IAPP amyloid. This suggests that the 8-20 region may play some defining role in the overall morphology of IAPP amyloid fibrils.

Factors modulating IAPP folding and fibrillogenesis

Our observations suggest that the N-terminal half of IAPP is composed of a relatively flexible component (residues ~1-8) and an amyloidogenic domain (residues ~8-20). The N-terminal region has a number of unique features that may influence the IAPP fibril-forming pathway. For example, this region contains a high density of electrostatic charge, a unique histidine residue in the human sequence and a disulphide bridge. To determine if these features regulate the folding of IAPP and its peptide fragments, we examined the pH-dependency of fibril formation, the effects of counterion shielding and oxidation state of the disulphide. Full-length IAPP contains only positively charged sites (Lys1, Arg11 and His18) and so is excluded from forming intra/intermolecular salt-bridges but these residues may modulate aggregation and/or folding. This may be most relevant to His18, which can alternate *in vivo* between its charged and uncharged states. Histidine residues are also sites for metal ion binding and have been shown to be involved in Aβ amyloid fibril assembly through electrostatic side-chain interactions (Atwood *et al*., 1998; Fraser *et al*., 1994).

To assess these factors, the conformation and fibril formation of full-length human IAPP was examined at acidic and alkaline pH (10 mM HCl or NaOH) in the absence of buffering ions. Aggregation into fibrils was observed at both extremes of pH but, as compared to neutral conditions, variations were observed in fibril morphology and protofilament ordering. CD spectra of IAPP at pH 2.4 showed a typical random to β transition over a period of 48 hours (Figure 5(a)). Negative stain EM indicated that this resulted in predominantly fine protofilaments that were arranged in ribbons or loosely wound into fibrillar aggregates (Figure 5(b)). At near neutral, pH 6.5, the

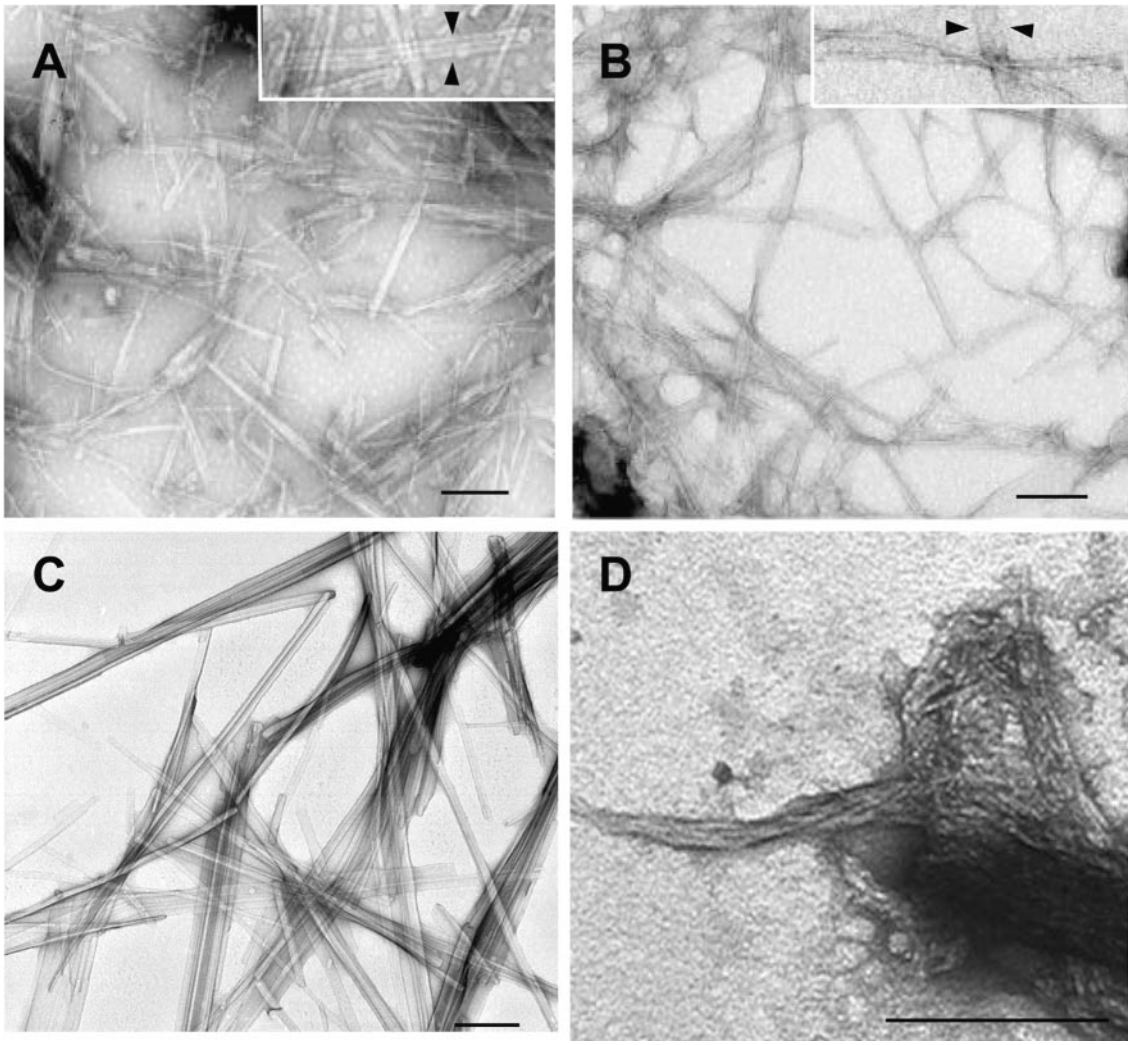

Figure 4. Electron micrographs of the IAPP fragments. (a) Human IAPP residues 8 to 20 (100 μg/ml) formed short laterally aligned fibrils that resulted in a ribbon-like morphology. These structures were produced by the association of individual protofilaments that were resolved at higher magnification (inset). (b) Comparable fibres were observed with the rat 8-20 sequence. (c) The overlapping fragment, IAPP 18-29, which also contained the amyloid domain, residues 20 to 29, formed laterally aligned rod-like fibrils. (d) The remaining C-terminal β-sheet domain, IAPP 30-37, formed short fibrils that were also accompanied by amorphous aggregates. Scale bars represent 200 nm, insets represent a 2× magnification relative to the main panels.

aggregation process was slowed to some degree with the CD spectrum indicating a β-sheet structure only after 65 hours of incubation (Figure 5(c)). However, the morphology of the fibrils was more typical, with long, unbranching fibres with a uniform diameter of 18-20 nm (Figure 5(d)).

Under basic conditions, pH 11.2, the CD spectra indicated an initial random coil that gradually attenuated in signal strength over the course of 48-96 hours incubation (Figure 5(e)). At high pH, IAPP is deprotonated completely and the precipitate was similar to that observed with the shorter hydrophobic 30-37 fragment, where fibril-like structures radiated from amorphous material (Figure 5(f)). As with IAPP 8-20, FTIR demonstrated that the aggregated peptide assembled into a β-sheet conformation (data not shown). These results demonstrate that, unlike other amyloid peptides such as Aβ, the folding and aggregation of IAPP occurs independent of electrostatic interactions. However, the morphological differences indicate that assembly of the protofilament subunits is affected by pH. This suggests that the charged side-chains within the N-terminal region may modulate interactions between protofilaments to produce the mature amyloid fibril. The role of charged residues is further illustrated by the effects of counterion shielding on peptide aggregation.

When reconstituted into 10 mM acetate buffer (pH 5.5), human IAPP 1-37 was maintained as a random coil for a period of 80-90 hours. This disordered state was gradually converted to the β-sheet conformation (Figure 6(a)). The fibrils formed under these conditions were typical of amyloid fibrils but were somewhat longer than those seen in water alone (Figure 6(b)). In addition, in the pre-

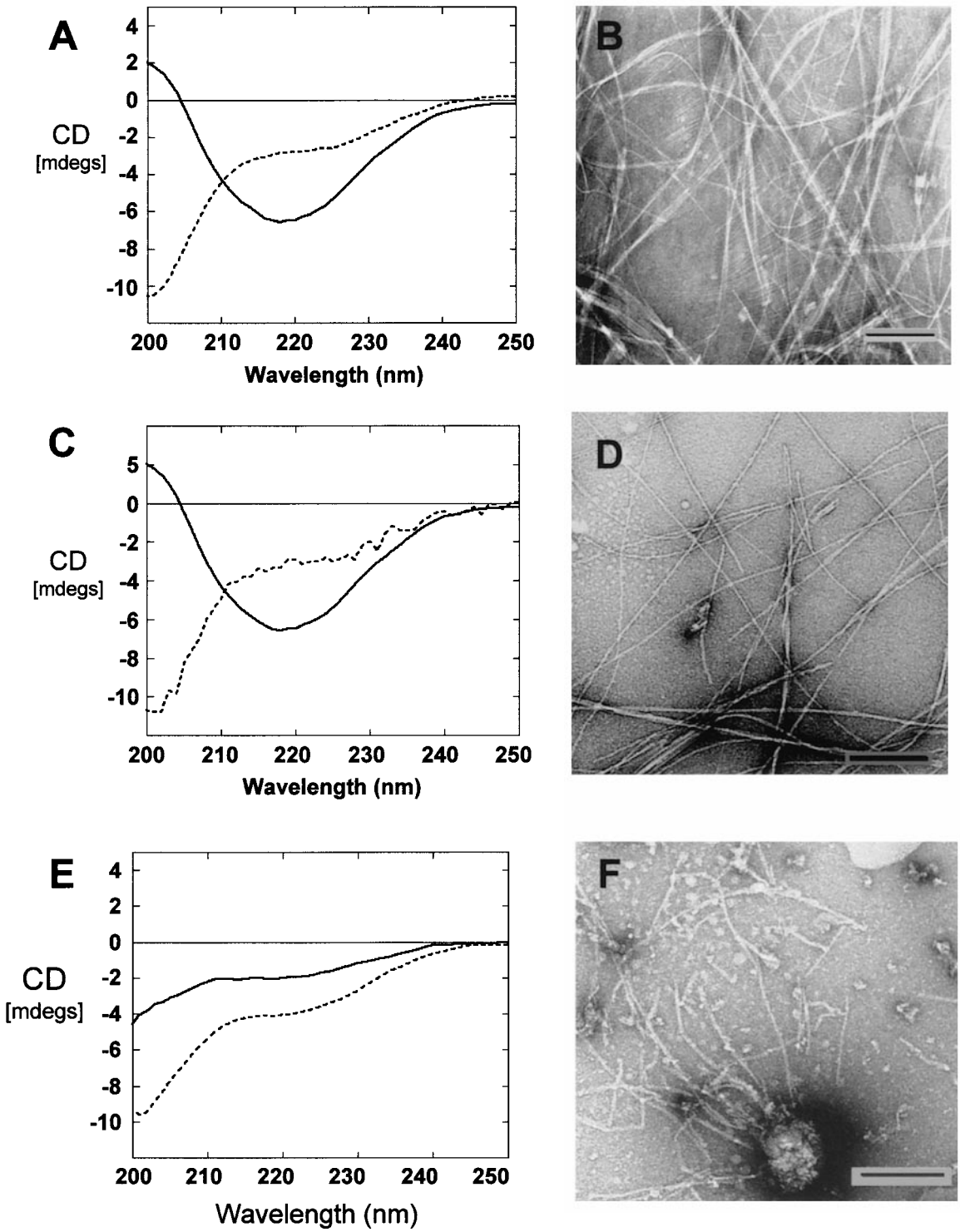

Figure 5. Conformation and fibril formation of IAPP as a function of pH. (a) IAPP 1-37 prepared at acid pH (2.4) underwent a random coil (broken line) to β-sheet (continuous line) conformational change over a period of 48 hours. (b) This resulted in the assembly of protofilaments that displayed lateral aggregation and loosely wound into fibrils. (c) IAPP at near neutral pH (6.7) showed a similar random to β-sheet transition but only following incubation for 72-96 hours. (d) Electron microscopy revealed typical amyloid fibrillar morphology. (e) At basic pH, 11.2, IAPP 1-37 was initially in a random coil conformation (broken line) and an attenuation of the signal (continuous line) was observed over 96 hours. (f) The aggregates formed under these conditions were amorphous and were associated with more poorly defined fibrils. Scale bars represent 200 nm.

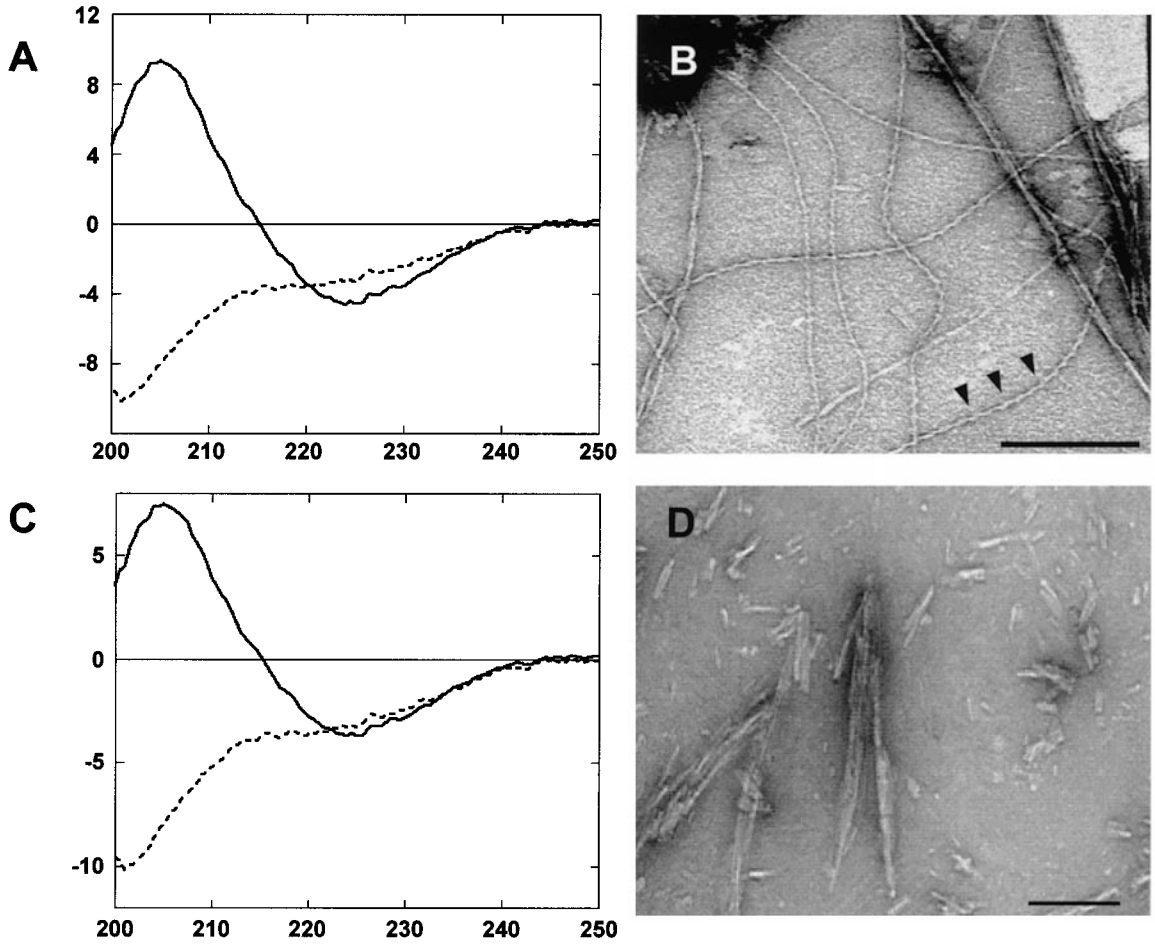

Figure 6. The effect of counter ions on IAPP folding and aggregation. (a) IAPP prepared in 10 mM sodium acetate (pH 5.5) was initially in random coil conformation (broken line) that gradually converted to a β-sheet (continuous line) following incubation for 80-90 hours. (b) The fibrils formed under these conditions were long and often displayed a helical twist (arrows). (c) Human IAPP prepared in 2 mM sodium citrate buffer (pH 5.5), was also initially random (broken line) but precipitated as a weaker β-sheet signal (continuous line) over a much more rapid time-course of three to four hours. (d) This accelerated aggregation resulted in short, fibrils with ragged ends that were not typical of amyloid fibrils. Scale bars represent 200 nm in (b) and 100 nm in (d).

sence of an acetate counterion, the IAPP fibrils exhibited a ''helical'' twisting not normally seen for the full-length peptide (Figure 6(b), arrowheads). In 2 mM citrate buffer at the same pH (5.5) there was an attenuation of the CD signal (after four hours) and the appearance of a weaker β-sheet minima (Figure 6(c)). This was associated with the appearance of ragged short fibrils with uneven ends (Figure 6(d)). The larger charge on the citrate ion could contribute to a shielding effect and reduced solubility. At neutral pH with Tris buffers, IAPP underwent a conversion to β-sheet more rapidly than in water alone, while phosphate buffers induced a rapid precipitation similar to that seen with citrate (data not shown).

The contributions of the oxidized disulphide was examined in both the intact IAPP 1-37 as well as the 1-13 peptide. As discussed, the 1-13 fragment containing an intact disulphide bridge, exhibited only random coil conformation even following long incubation periods (more than five weeks). When examined under strong reducing conditions (100 mM DTT), no change in the folding or aggregation state of the N-terminal 1-13 fragment was observed (data not shown). It was assumed that the IAPP disulfide was fully reduced under these strong conditions but any residual intact bridges were not quantified directly. More importantly, full-length human IAPP still assembled into a β-sheet conformation under these conditions and no difference in fibril morphology was observed.

Discussion

Here, we demonstrate a previously unrecognised amyloidogenic domain in hIAPP, which, as a peptide fragment is capable of forming fibrils in a β-conformation. This region, hIAPP 8-20, is in the central, largely conserved region of the molecule. Furthermore, the comparable rat fragment, which

has an arginine substitution at position 18 but is otherwise homologous to human IAPP 8-20, also formed fibrils. This newly identified β-strand region in addition to the two previously described amyloidogenic domains, hIAPP 20-29 and 30-37 (Betsholtz *et al*., 1989; Nilsson & Raleigh, 1999; Westermark *et al*., 1990), could have a role in intermolecular interactions to form oligomers as well as interacting to form a triple-stranded intramolecular β-sheet. The results of our study also suggest that the region between 1 and 7 is not essential for fibril formation. However, it is possible that these flexible residues may modulate fibril formation in a manner similar to that observed for the Aβ peptide. In this case, truncation of the N terminus (Aβ 10-40 or 10-42) actually produced a more amyloidogenic peptide (Hilbich *et al*., 1992). Detailed kinetic studies comparing full-length IAPP and the IAPP 8-37 fragment (or other truncated peptides) would be necessary before this possibility could be fully resolved.

The native structure of IAPP has yet to be determined but current data suggest that the free peptide exists *in vivo* in a random structure (Plaxco & Gross, 1997; Higham *et al*., 2000). Under certain *in vivo* conditions, as yet unidentified, hIAPP adopts a β-sheet structure and forms amyloid fibrils. Rodent IAPP does not form amyloid fibrils *in vivo* or *in vitro* (Westermark *et al*., 1990). This is the first report of a fragment of rat IAPP (rat IAPP 8-20) forming fibrils. Since the 30-37 domain of rat IAPP is identical with the human sequence and capable of forming fibrils, it is possible that these two β-strands could associate to promote rat IAPP aggregation. However, as indicated previously, the proline substitutions in the rodent peptide likely preclude the transition to a complete amyloid fibril. The other more obvious intrinsic factors associated with the human sequence of IAPP appear to have little impact on fibril formation. The histidine residue and the disulphide bridge are not essential for *in vitro* fibrillogenesis. Fibril morphology was affected by pH, with fibril assembly being mostly in the form of protofilaments under acidic conditions, suggesting that lateral association of protofilaments is influenced by charged residues.

A model for IAPP conversion to β-sheet oligomers

The presence of three potential β-strands in the hIAPP sequence suggests that an intramolecular β-sheet can be formed. A β-turn has been predicted at Asn31, which would result in two adjacent β-strands, 32-37 and 24-29, creating an antiparallel β-sheet. The third β-strand contained in the fragment 8-20 could extend this sheet with a turn in the region 18-23 (predicted at serine 20). This assembly may be stabilised by side-chain hydrogen bonding between the uncharged polar side-chains of the six asparagine residues as well as other uncharged polar residues including glutamine, serine and threonine. The process of fibril assembly could be driven by hydrophobic interactions. Ten of the 37 residues in hIAPP are hydrophobic, and increased hydrophobicity driving the initial stages of fibril formation has been demonstrated (Kayed *et al*., 1999), suggesting that protofilament and fibril assembly expose hydrophobic regions.

Human IAPP formed fibrils at acidic and neutral pH, suggesting that a change in charge is not an essential feature for fibrillogenesis. Moreover, *in vivo*, the transition of IAPP from the β-cell secretory granule (pH 5.5) to the extracellular space (pH 7.4) is unlikely to have a significant effect on the conformation of the peptide. It is more probable that changes in the granule components and/or in the extracellular environment, which are unique to type 2 diabetes, promote fibril formation. Metabolic or post-translational changes (e.g. glycosylation or aberrant proteolysis) that promote seeding of amyloidogenic fragments or conformational rearrangements could initiate amyloid deposition. However, the role of these pathways has yet to be fully investigated. The β-cell granule contains more than 30 proteins and has high concentrations of both zinc and calcium (Emdin *et al*., 1980; Hutton, 1994). Intracellular molecular crowding within the granule compartment could be essential for the maintenance of hIAPP in its native conformation or inhibition of aggregation, as has been shown for other peptides (van den Berg *et al*., 1999). Disease-related changes in the extracellular space in the early stages of type 2 diabetes due to hypersecretion of insulin, IAPP and related peptides from the β-cells could result in a local increased concentration of hIAPP and aggregation, leading to fibril formation.

Materials and Methods

Peptide synthesis and supply

Synthetic human IAPP (1-37) was purchased from Bachem (UK), human IAPP (8-37), (20-29) and (1-13) were purchased from Peninsula Laboratories (St Helens, UK). Human IAPP (8-20), (18-29), (30-37) and rat IAPP 8-20 were synthesized on an Applied Biosystems 430A Automated Peptide Synthesiser using standard Fmoc methodology. The peptides were purified by reverse phase HPLC using water/acetonitrile mixtures buffered with 0.1% (v/v) trifluoroacetic acid, on a POROS 20R2 column of 10 mm × 250 mm at a flow rate of 15 ml/minute. All peptides were prepared by the same method to ensure similar ''histories'' of protein folding. The synthetic peptides were solubilised in 100% HFIP (1 mg/ml), filtered (0.2 μm), divided into aliquots and lyophilised (Higham *et al*., 2000). Aliquots were reconstituted as required. Buffers were prepared in sterile, distilled, deionised water and included 10.0 mM sodium acetate (pH 5.5), 2.0 mM sodium citrate (pH 5.5), 2.0 mM sodium phosphate (pH 7.4), and 2.0 mM Tris- HCl (pH 7.4) (all chemicals from Sigma Aldrich, Poole, UK). Samples were also incubated in water with addition of 10 mM HCl or 10 mM NaOH to examine the effect of pH in the absence of counter ions.

CD spectroscopy

Spectra (average of five scans) were collected from samples (200 μl) at 0.5 nm intervals between wavelengths of 180 nm and 260 nm using a Jasco J720 spectropolarimeter and quartz cuvettes (Hellma (England) Limited, UK) with a 1 mm path-length. Multiple samples were examined under all conditions. The polarimeter voltage was monitored to ensure that solutions were transparent. Samples were incubated at 20 °C and a baseline spectrum (buffer/water only) was subtracted from collected data.

Electron microscopy

Each sample prepared for CD was examined using transmission electron microscopy. Aliquots (3 μl) were applied to formvar and carbon-coated grids, which had been rendered hydrophilic by exposure to UV radiation. The samples were incubated on the grid for ten minutes at room temperature, excess material blotted off, and stained for ten minutes with 2 % (w/v) uranyl acetate in water. Excess uranyl acetate was blotted off and the sample left to air-dry. All samples were examined using a Jeol JEM1010 electron microscope with an accelerating voltage of 80 kV.

Fourier-transform infrared spectroscopy

Exchangeable hydrogen atoms were replaced by deuterium atoms by dissolving peptides in ^2H_2O (1 mg/ml), incubating the sample at 50 °C for 30 minutes followed by drying the sample in a speed vacuum. This procedure was repeated three times. The deuterated peptides were incubated for four weeks at 50 °C. Samples were microfuged at 13,000 rpm for two minutes and the visible precipitate was resuspended in 25 μl of ^2H_2O and examined. IR spectra were recorded with an FTS-175C Fourier-transform spectrophotometer (BioRad, UK) equipped with a liquid nitrogen-cooled mercury/cadmium telluride detector and purged with a continuous flow of nitrogen gas. Samples (25 μl) were inserted between CaF_2 windows using a 50 μm mylar spacer. A total of 250 interferograms were recorded at room temperature with a spectral resolution of 2 cm^{-1}. For each spectrum, water vapour was subtracted and baseline corrected. For all spectra, the area between 1590 and 1710 cm^{-1} was normalised to unity. Second derivatives of the amide I band spectra were produced to determine the wavenumbers of the different spectral components.

Fibre X-ray diffraction

Peptides were dissolved in filtered (0.22 μm) deionised water at 10 mg/ml and incubated for two weeks at 37 °C. A droplet of this solution was suspended between two wax-filled capillaries and left to dry. The stalk of dried material was examined. X-ray diffraction patterns were collected using a Rigaku rotating anode X-ray source and an MAR research image plate or using the Grenoble synchrotron source. The images were examined using ipmosflm (CCP4) run on a Dec alpha workstation.

Thioflavin S staining

Thioflavin S (Sigma) was made up to 0.5 % (w/v) in distilled, deionized water and filtered. Human IAPP 1-37 and fragments, 8-20, 18-29, 20-29, 30-37 and rat 8-20 were dried in 10 μl aliquots onto glass microscope slides. Thio-S was applied to the slides for one to two minutes, rinsed with 70 % (v/v) ethanol followed by a water wash. Samples were mounted with Citifluor (Agar Scientific, Stanstead, UK) in PBS/glycerol and viewed with a fluorescence microscope.

Acknowledgements

We are grateful to the following for financial support; the British Diabetic Association (E.J. and C.H.), the Mary Mackenzie Bequest (E.J.), the Wellcome Trust (A.C.), the Ontario Mental Health Foundation (P.E.F.) and the Alzheimer's Society of Ontario (P.E.F.). Funding was also provided to P.E.F. by Neurochem. Inc. (Montréal, Québec). L.C.S. is a Wellcome RCDF, M.G. was funded by a BBSRC David Phillips research fellowship and J.Z. was supported by the European Commission and Wellcome Trust. This work was supported by a Wellcome International Collaborative Research Grant (A.C. and P.E.F.). The Jeol Electron Microscope in the Department of Human Anatomy, Oxford was purchased with a grant from the Wellcome Trust. We thank Bjarne Rasmussen from ESRF Grenoble for assistance with collection of the diffraction data.

References

Atwood, C. S., Moire, R. D., Huang, X., Scarpa, R. C., Bacarra, N. M. E., Romano, D. M., Hartshorn, M. A., Tanzi, R. E. & Bush, A. I. (1998). Dramatic aggregation of Alzheimer Abeta by Cu(II) is induced by conditions representing physiological acidosis. *J. Biol. Chem.* **273**, 12817-12826.

Betsholtz, C., Christmansson, L., Engström, U., Rorsman, F., Svensson, V., Johnson, K. H. & Westermark, P. (1989). Sequence divergence in a specific region of islet amyloid polypeptide (IAPP) explains differences in islet amyloid formation between species. *FEBS Letters,* **251**, 261-264.

Betsholtz, C., Christmanson, L., Engström, U., Rorsman, F., Jordan, K., O'Brien, T. D., Murtaugh, M., Johnson, K. H. & Westermark, P. (1990). Structure of cat islet amyloid polypeptide and identification of amino acid residues of potential significance for islet amyloid formation. *Diabetes,* **39**, 118-122.

Clark, A., Cooper, G. J., Lewis, C. E., Morris, J. F., Willis, A. C., Reid, K. B. & Turner, R. C. (1987). Islet amyloid formed from diabetes-associated peptide may be pathogenic in type-2 diabetes. *Lancet,* **ii**, 231-234.

Deleage, G. & Roux, B. (1987). An algorithm for protein secondary structure prediction based on class prediction. *Protein Eng.* **1**, 289-294.

Emdin, S. O., Dodson, G. G., Cutfield, J. M. & Cutfield, S. M. (1980). Role of zinc in insulin biosynthesis. Some possible zinc-insulin interactions in the pancreatic β-cell. *Diabetologia,* **19**, 174-182.

Fraser, P. E., Nguyen, J., Surewicz, W. & Kirschner, D. A. (1991). pH-Dependent structural transitions of Alzheimer amyloid-β/A4 peptides. *Biophys. J.* **60**, 1190-1201.

Fraser, P. E., McLachlan, D. R., Surewicz, W. K., Mizzen, C. A., Snow, A. D., Nguyen, J. T. & Kirschner, D. A. (1994). Conformation and fibrillo-

genesis of Alzheimer Aβ peptides with selected substitution of charged residues. *J. Mol. Biol.* **244**, 64-73.

Glenner, G. G., Eanes, E. D. & Wiley, C. A. (1988). Amyloid fibrils formed from a segment of the pancreatic-islet amyloid protein. *Biochem. Biophys. Res. Commun.* **155**, 608-614.

Griffiths, J. M., Ashburn, T. T., Auger, M., Costa, P. R., Griffin, R. G. & Lansbury, P. T. (1995). Rotational resonance solid-state NMR elucidates a structural model of pancreatic amyloid. *J. Am. Chem. Soc.* **12**, 3539-3546.

Higham, C. E., Jaikaran, E. T. A. S., Fraser, P. E., Gross, M. & Clark, A. (2000). Preparation of synthetic human islet amyloid polypeptide (IAPP) in a stable conformation to enable stucy of conversion to amyloid-like fibrils. *FEBS Letters,* **470**, 55-60.

Hilbich, C., Kisters-Woike, B., Reed, J., Masters, C. L. & Beyreuther, K. (1992). Substitutions of hydrophobic amino acids reduce the amyloidogenicity of Alzheimer's disease βA4 peptides. *J. Mol. Biol.* **228**, 460-473.

Hubbard, J. A. M., Martin, S. R., Chaplin, L. C., Bose, C., Kelly, S. M. & Price, N. C. (1991). Solution structures of calcitonin-gene-related-peptide analogs of calcitonin-gene-related peptide and amylin. *Biochem. J.* **275**, 785-788.

Hutton, J. C. (1994). Insulin secretory granule biogenesis and the proinsulin-processing endopeptidases. *Diabetologia,* **37**, S48-S56.

Kayed, R., Bernhagen, J., Greenfield, N., Sweimeh, K., Brunner, H., Voelter, W. & Kapurniotu, A. (1999). Conformational transitions of islet amyloid polypeptide (IAPP) in amyloid formation *in vitro. J. Mol. Biol.* **287**, 781-796.

McLean, L. R. & Balasubramaniam, A. (1992). Promotion of beta-structure by interaction of diabetes associated polypeptide (amylin) with phosphatidylcholine. *Biochim. Biophys. Acta,* **1122**, 317-320.

Nilsson, M. & Raleigh, D. (1999). Analysis of amylin cleavage products provides new insights into the amyloidogenic region of human amylin. *J. Mol. Biol.* **294**, 1375-1385.

Plaxco, K. W. & Gross, M. (1997). Cell biology. The importance of being unfolded. *Nature,* **386**, 657-659.

Roberts, A., Leighton, B., Todd, J., Cockburn, D., Schofield, P., Sutton, R., Holt, S., Boyd, Y., Day, A. & Foot, E., *et al.* (1989). Molecular and functional characterization of amylin, a peptide associated with type 2 diabetes mellitus. *Proc. Natl Acad. Sci. USA,* **86**, 9662-9666.

Röcken, C., Linke, R. P. & Saeger, W. (1992). Immunohistology of islet amyloid polypeptide in diabetes mellitus: semi-quantitative studies in a post-mortem series. *Virchows Arch. A Pathol. Anat. Histopathol.* **421**, 339-344.

Saldanha, J. & Mahadevan, D. (1991). Molecular model-building of amylin and alpha-calcitonin gene-related polypeptide hormones using a combination of knowledge sources. *Protein Eng.* **4**, 539-544.

Schneider, H. M., Storkel, S. & Will, W. (1980). Das amyloid der Langerhansschen inseln und seine beziehung zum diabetes mellitus. *Dtsch med Wschr.* **105**, 1143-1147.

Schwartz, P. (1970). *Amyloidosis, Causes and Manifestation of Senile Deterioration*, Thomas, Springfield, IL.

Sunde, M., Serpell, L. C., Bartlam, M., Fraser, P. E., Pepys, M. B. & Blake, C. C. F. (1997). The common core structure of amyloid fibrils by synchrotron X-ray diffraction. *J. Mol. Biol.* **273**, 729-739.

Surewicz, W. K., Mantsch, H. H. & Chapman, D. (1993). Determination of protein secondary structure by fourier transform infrared spectroscopy: a critical assessment. *Biochemistry,* **32**, 189-394.

van den Berg, B., Ellis, J. & Dobson, C. M. (1999). Effects of macromolecular crowding on protein folding and aggregation. *EMBO J.* **18**, 6927-6933.

Westermark, P. & Johnson, K. H. (1988). The pathogenesis of maturity-onset diabetes mellitus: is there a link to islet amyloid polypeptide? *Bioessays,* **9**, 30-33.

Westermark, P., Wilander, E., Westermark, G. T. & Johnson, K. H. (1987). Islet amyloid polypeptide-like immunoreactivity in the islet B cells of type 2 (non-insulin-dependent) diabetic and non-diabetic individuals. *Diabetologia,* **30**, 887-892.

Westermark, P., Engstrom, U., Johnson, K. H., Westermark, G. T. & Betsholtz, C. (1990). Islet amyloid polypeptide: pinpointing amino-acid-residues linked to amyloid fibril formation. *Proc. Natl Acad. Sci. USA,* **87**, 5036-5040.

Edited by F. E. Cohen

(Received 9 February 2001; accepted 12 February 2001)